

Analysis and Test on Step Surmounting Performance of a W-Shaped Track Robot

Yunwang Li*, Xucong Yan, Feng Tian, Delong Zhao and Bin Li

School of Mechanical and Electrical Engineering, China University of Mining and Technology, Xuzhou, China

Abstract: The step surmounting performance of a mobile robot is an important performance measure for obstacle-navigation. In this paper, a W-shaped track robot is taken as a research object and the step-climbing performance is analyzed theoretically. It is simulated by the RecurDyn software and is tested on a terrain simulation platform using a NDI dynamic measuring machine. In the independent step climbing process, the robot's front track sections of W-shaped track climb up the nosing of the step firstly and then the rear ones climb. Once the robot's position of center of gravity climbs over the nosing, the robot will climb up easily. According to different riser heights and positions of center of gravity, there are two situations for the climb of the rear tracks: (1) if the gravity center has been over the nosing when the rear tracks touch the nosing, then the robot's rear tracks will climb the steps softly without any impact; (2) and if not, then the robot's front tracks will rise and, then fall causing an impact. It is very easy for the robot to climb the step with a slope because of the guiding role of the slope. The robot can easily climb up the steps which are less than 240mm high, and the maximum tested step height is 320mm, but there should be a lower step in front of the step, and the robot's gravity center should be adjusted to a very low and forward position. In short, the W-shaped track mobile robot has a good performance for the overcoming of structured terrains.

Keywords: Dynamic measurement system, Gravity center position, Step surmounting, W-shaped track robot.

1. INTRODUCTION

Mobile robots for environment exploration, disaster rescue and military reconnaissance need good terrain maneuverability and adaptability, because they might have to face and try to surmount all types of obstacles [1-5]. Obstacle-overcoming performance is an important index to evaluate the robot. Some obstacle terrain can be simplified to step. The step surmounting performance of the robot is an important performance measure of obstacle-navigation performance. A rocker type asymmetrical W-shaped track robot for coal mine exploring was designed and its prototype was built [6, 7]. The robot has good passive adaptability for rough terrain environments [8]. In this paper, in order to study the motion characteristics of the W-shaped track moving mechanism, theoretical analysis and simulation is performed by the RecurDyn software. The step climbing capacities are tested on a terrain simulation platform using NDI dynamic measuring machine which can track the important positions and motions of the robot during its step climbing. Then step overcoming performance of the W-shaped track robot is analyzed.

2. ROCKER-TYPE W-SHAPED TRACK ROBOT AND ITS PHYSICAL DIMENSIONS

The rocker type W-shaped track robot is shown in Fig. (1). It is comprised of two asymmetrical W-shaped rocker

track suspensions, a differential mechanism and a main body. The two track suspensions are hinged coaxially with the main body. Each suspension is comprised of a front and a rear track assembly which is connected by a chain transmission, and there is a tensioner idle outside each track assembly. The track suspensions are driven by DC motors installed in the main body. The link rod's type is differential mechanism which links the main body and the two suspensions. The suspensions will rock with the rough terrain during the robot's deployment in the unstructured environment. But in a structured terrain, the track suspensions and the main body will remain fixed with the whole structure. The four track assemblies sections of the track can be assigned as track 1, 2, 3 and 4, respectively. The wheels of the track suspensions can be assigned as wheel 1, 2, 3, 4 and 5, respectively as shown in Fig. (1). The robot's physical dimensions are marked in Fig. (2) and are listed in Table 1.

3. TEST SYSTEM CREATING

A test system is created using the NDI Dynamic Measuring Machine (DMM) and a terrain simulation platform. The DMM can track the markers which are the specific points of interest on the robot [9]. The test system and the positions of imaginary markers were introduced in reference [8]. The terrain simulation platform is made up of a parallelogram adjustable platform and a fixed trapezoidal platform, as shown in Fig. (3). The height of the parallelogram adjustable platform can be adjusted from 270mm to 450mm. The fixed trapezoidal platform includes a 270mm-high independent step and a step with 45° slope.

*Address correspondence to this author at the Daxue Road, Xuzhou, China. Postcode: 221116; Tel: (86)18605168277; E-mail: yunwangli@cumt.edu.cn

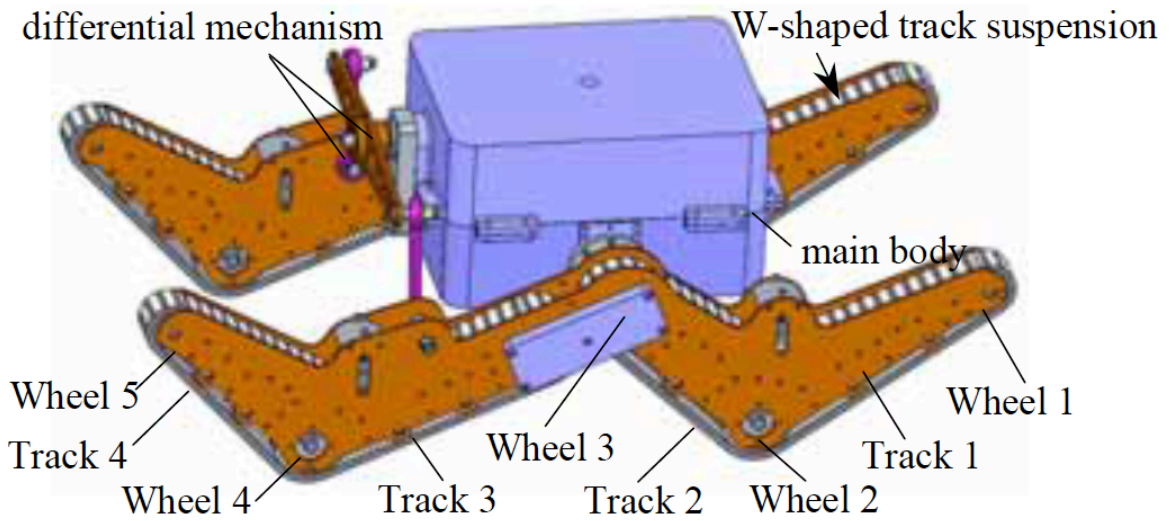


Fig. (1). Mechanical structure of the rocker-type W-shaped track robot.

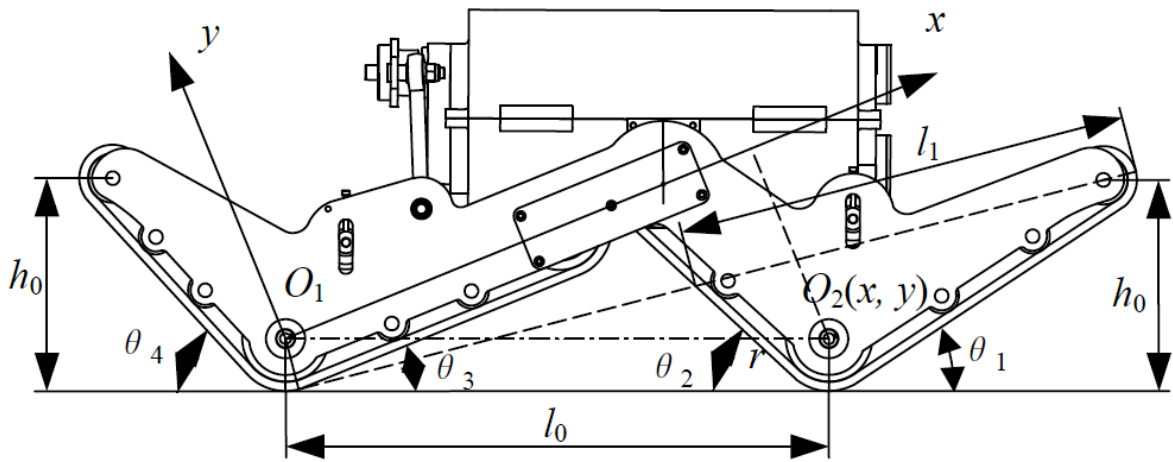


Fig. (2). Physical dimensions of the robot.

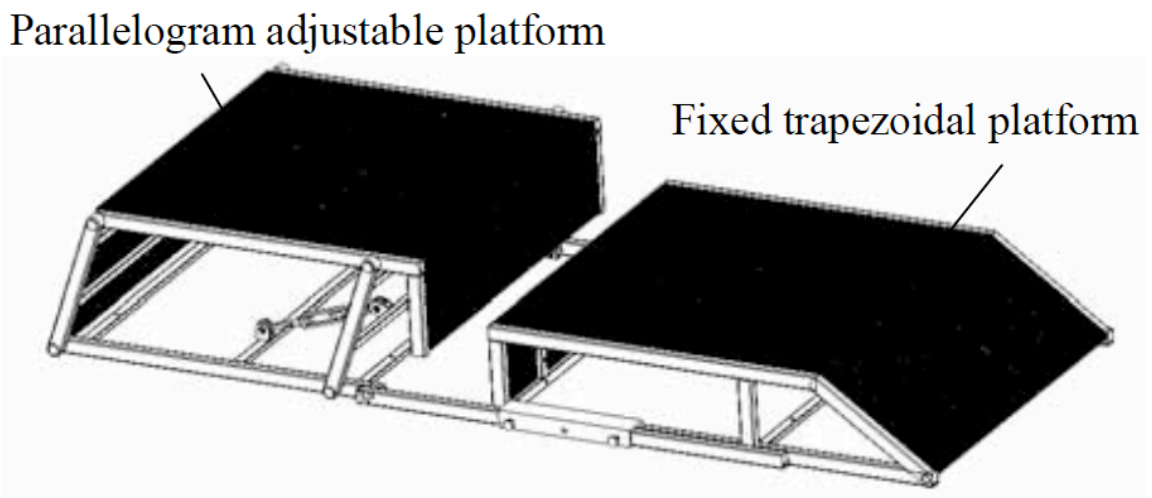


Fig. (3). A terrain simulation platform.

Table 1. Physical dimensions of the robot.

Item Names	Radius of the Touchdown Wheel (Including the Track Thickness)	Lifting Height of the Tracks	Track Wheels Touchdown Length	Length of a Transversal Serif	Initial Elevation of Track 3	Initial Elevation of Track 1	Coordinate Values of Wheel 3 Center O_2 in Fig. (2)	Gravity Center Coordinates (can be Adjusted)
Signs	r (mm)	h_0 (mm)	l_0 (mm)	l_1 (mm)	θ_1 ($^\circ$)	θ_3 ($^\circ$)	$O_2(x, y)$ (mm)	$G(x, y)$ (mm)
Numerical values	58	240	600	500	33.4	22.2	$O_2(554.8, -226.6)$	$G(480, 24.8)$

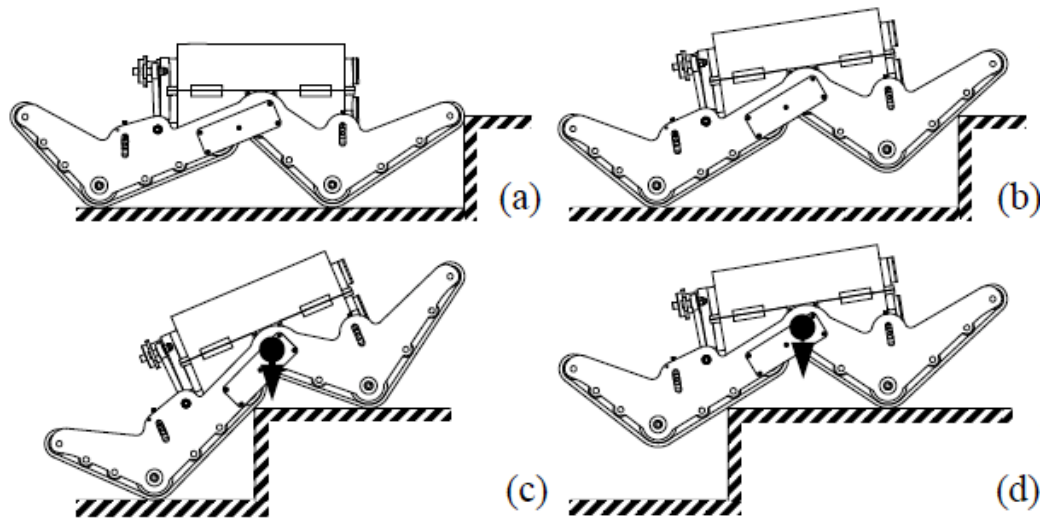


Fig. (4). Step-climbing process of the robot.

4. STEP CLIMBING

4.1. Analysis on the Step Climbing [10]

The height of the step which the robot can climb up has a relation with the friction coefficient between the tracks and the steps, the driving power, the position of the center of gravity of the robot and the shape and size of the track mechanism. In this paper, the influence of the shape and size of the track and the position of the center of gravity are discussed.

The first stage of the step-climbing process of the robot mobile platform is that the front tracks 1 and 2 climb over the nosing of the step, as shown in Fig. (4a, b). In the first stage, if the step is not too high the front tracks can climb the nosing with the help of the first inclined track sections. If the step is too high for the robot's front track to touch the step's nosing, then the robot's front tracks have to climb the riser of the step though it is very difficult. But in some special occasions, if there is a lower step just like a "foot pad" in front of the step. When the robot's front tracks climb on the "foot pad", the robot has an advantage of a certain elevation angle and the front tracks can contact the nosing, as shown in Fig. (5).

The second step-climbing stage is that the rear tracks 3 and 4 climb over the nosing. For a different step height, the

second climbing action is different. After the first climbing stage, the robot moves forward, then track 3 touches the nosing. If robot's center of gravity has crossed the nosing of the step, the robot can easily climb up the step with its front tracks contacting the step's upper horizontal plane as shown in Fig. (4c, d). The maximum height of the step the robot can climb when the front touchdown wheels touch the upper plane is shown in Fig. (6). In this situation, the height that the robot could overcome is given by the equation (1) and (2), then equation (3) can be obtained. The value of α can be computed, then the maximum height of the step H_{max1} can also be obtained.

$$H(\alpha) = r + x \sin \alpha + y \cos \alpha - \frac{y+r}{\cos \alpha} \quad (1)$$

$$H(\alpha) = x_{o_2} \sin \alpha + y_{o_2} \cos \alpha \quad (2)$$

$$r + (x - x_{o_2}) \sin \alpha + (y - y_{o_2}) \cos \alpha - \frac{y+r}{\cos \alpha} = 0 \quad (3)$$

If robot's center of gravity has not crossed the nosing of the step then the elevation angle of track 3 will increase and the robot's wheel 2 will lift and leave the upper horizontal plane during the climb. When the center of gravity has crossed the nosing of the step, the robot will rotate to the

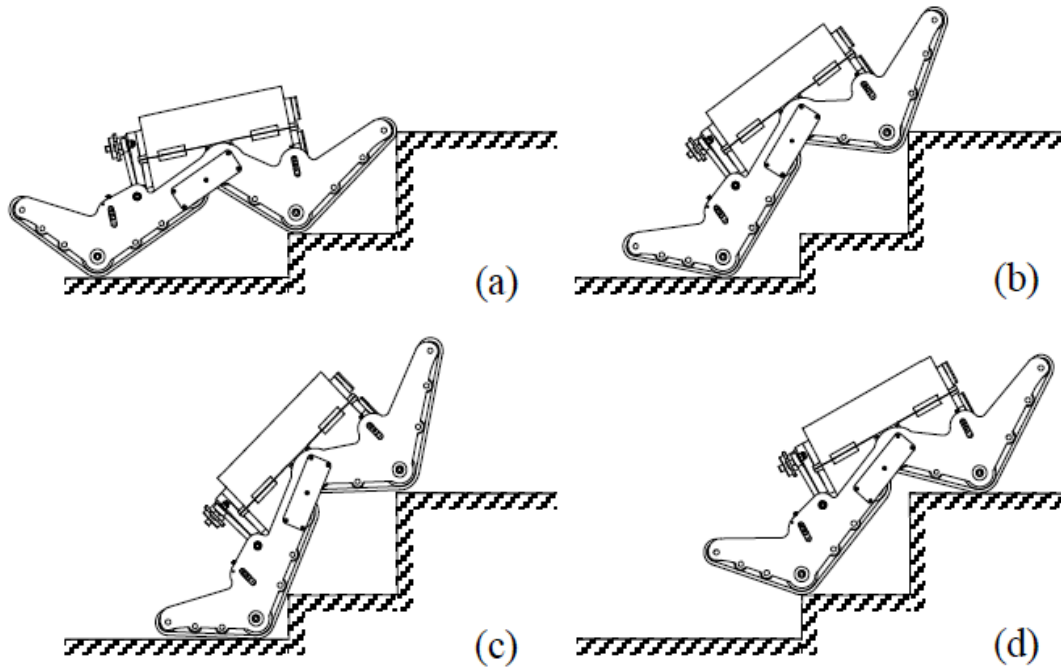


Fig. (5). Step with a "foot pad" climbing process of the front tracks.

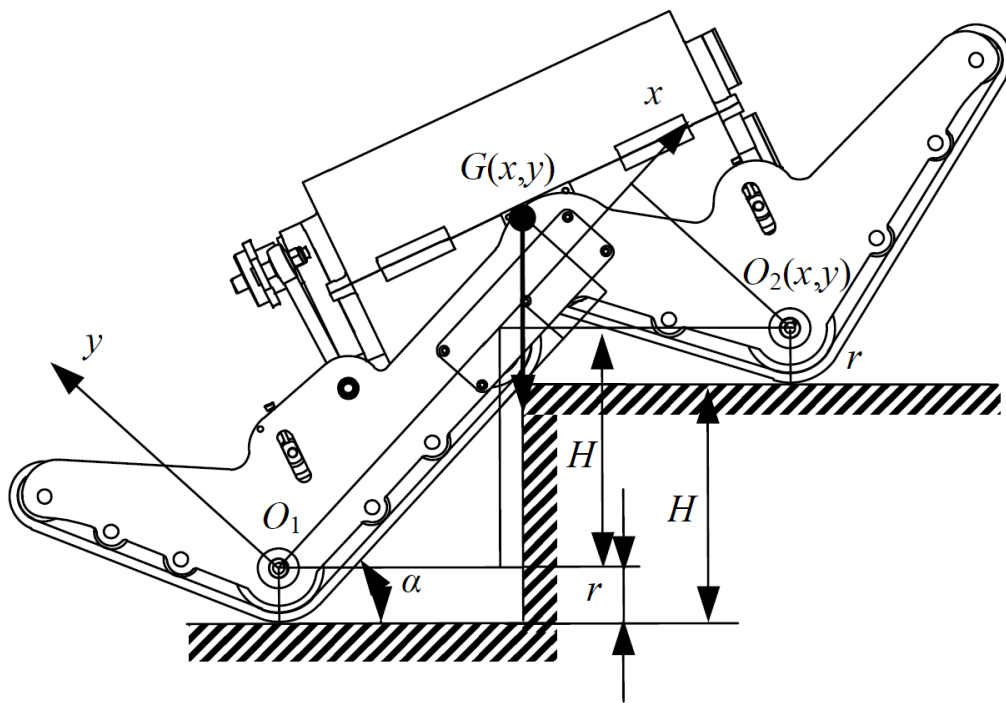


Fig. (6). The maximum height of the step the robot can climb with the front touchdown wheels contacting the upper plane.

upper plane again with the nosing as axis of rotation, shown in Fig. (7). Equation (1) is equally applicable to this situation, the first and second partial derivatives of α are given by

$$\frac{\partial H}{\partial \alpha} = x \cos \alpha - y \sin \alpha - \frac{(y+r) \sin \alpha}{\cos^2 \alpha} \quad (4)$$

$$\frac{\partial^2 H}{\partial \alpha^2} = -x \sin \alpha - y \cos \alpha - (y+r) \cdot \frac{\sin^2 \alpha + \cos \alpha}{\cos^3 \alpha} \quad (5)$$

$a \in (0, \frac{\pi}{2})$, $\frac{\partial^2 H}{\partial \alpha^2} < 0$, so the maximum value of function $H(\alpha)$ exists. When, $\frac{\partial H}{\partial \alpha} = 0$, $H(\alpha)$ has the maximum val-

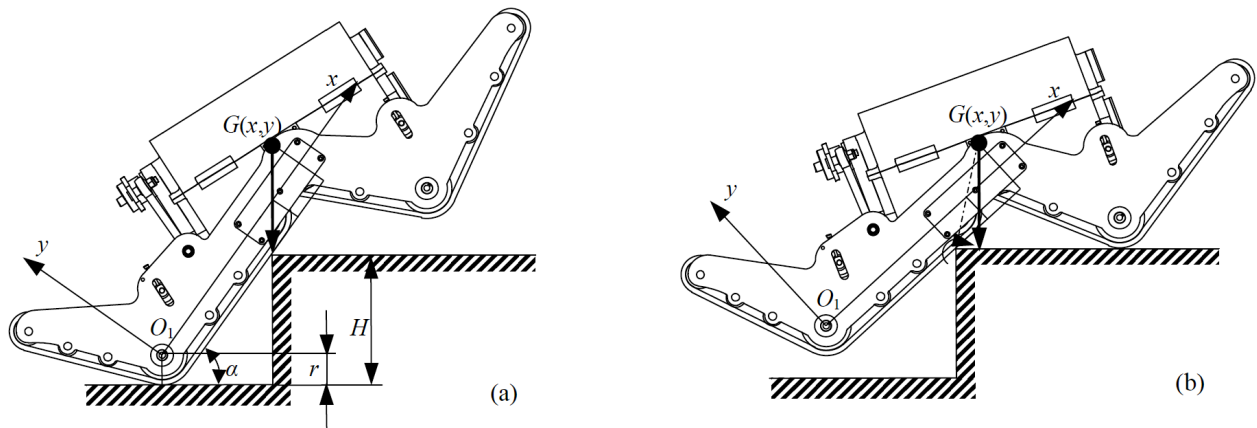


Fig. (7). High step climbing process of the rear tracks.

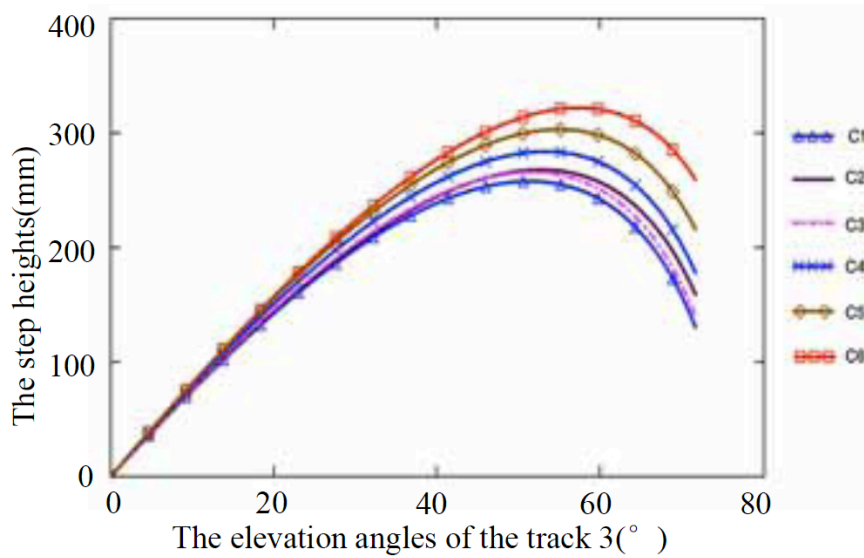


Fig. (8). Relation curves of the step height and rear tracks elevation angles according to different gravity center position.

Table 2. The step heights which the robot can overcome with different gravity center.

Gravity Center Position	G(450, 60)	G(450, 50)	G(460, 55)	G(470, 50)	G(480, 40)	G(480, 24.8)
H_{max1} (mm)	255.4	265.1	268.9	282.7	302.1	320.5
H_{max2} (mm)	258	268	270.1	284	303.3	322.1
Corresponding Curve in Fig. (9) of H_{max2}	C1	C3	C2	C4	C5	C6

ue H_{max2} which is the maximum height of the step which the robot can climb up.

Once the robot has been manufactured, the shape and size will be fixed. However, the position of center of gravity may change with the load and equipment's changing. The position of center of gravity of the robot exercises a great influence on the step-overcoming performance. So a reasonable design of the position of center of gravity is very important. Fig. (8) shows the relation curves of the step height

and rear tracks elevation angles according to different positions of center of gravity. Table 2 shows the effect of positions of center of gravity on the height of the step which the robot can climb up.

The robot can easily climb up a 240mm-high step, the nosing of which can be touched by its front tracks. If the step height is more than 240mm and there is no "foot pad" before the step, then the robot's front tracks will climb up the nosing by climbing the riser, which is in the same manner as vertical wall climbing.

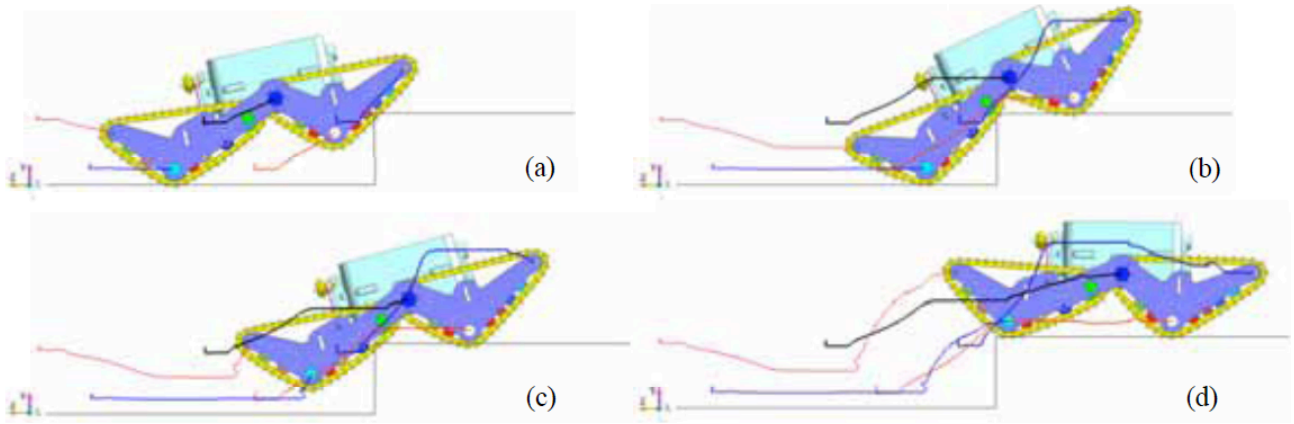


Fig. (9). Simulation of Independent Step Climbing using RecurDyn software.

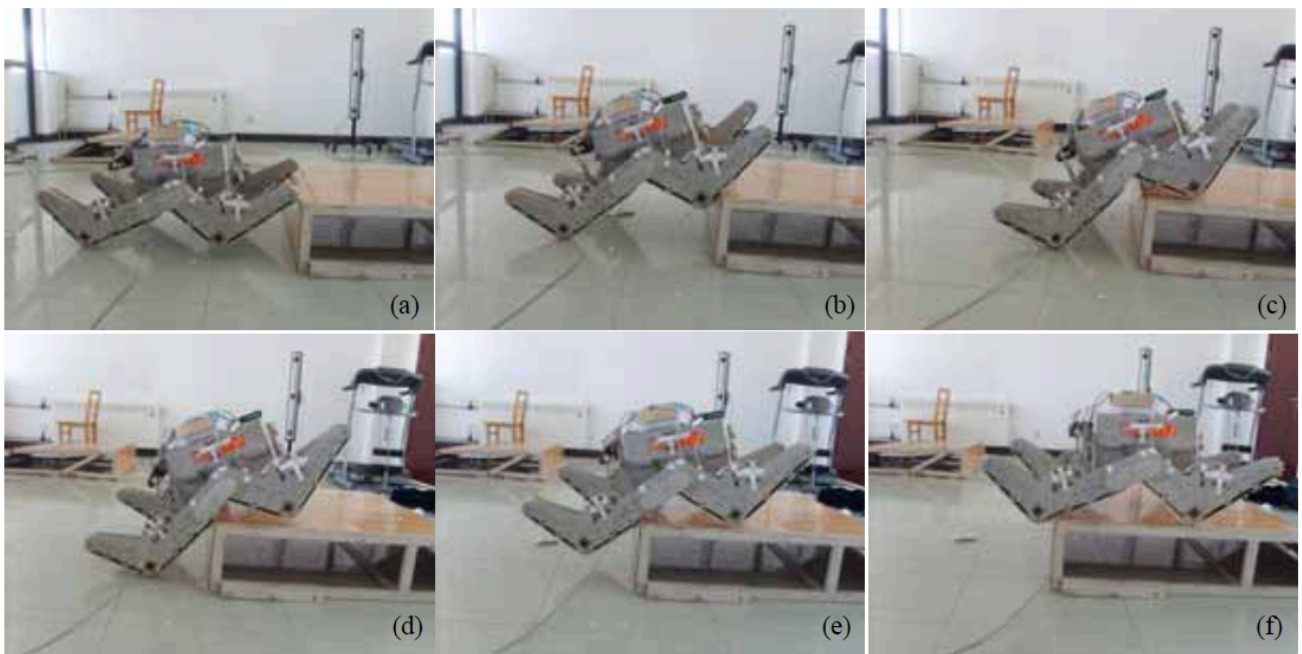


Fig. (10). Independent Step climbing test

4.2. Simulation and Test of Independent Step Climbing

4.2.1. Simulation of Independent Step Climbing

The 3D model of the robot is imported into the RecurDyn software, the process of robot's independent step climbing is simulated using the RecurDyn software [11]. In the simulation system, the Y coordinate direction is vertical direction. The 260 mm-high step climbing simulation process is shown in Fig. (9). The Y axis coordinate curves of the five wheels are drawn during the climbing process. The position of wheel 3 in Y coordinate direction is very close to the positions of center of gravity of the robot. The Y axis coordinate curve of wheel 3 reflects the trajectory of the robot's center of mass. Compared with the other curves, the curve is very smooth.

4.2.2. Test of Independent Step Climbing

In the laboratory, a 270 mm high step test platform is used to carry out the step climbing test. 270mm is too high for the robot's front tracks to contact the nosing of the step, the height of which is only 240mm. The floor and the riser are very smooth, so it adds to the difficulty for climbing for the robot. In order to make the front tracks touch the nosing, the front robot end is lifted and the upper ends of the robot's front tracks are propped up on the step nosing, as shown in Fig. (10a). In the test process, the robot climbed up the step then moved in reverse and climbed down the step. The positions of the markers and imaginary markers on the robot have been tracked and their three-dimensional coordinates have been recorded, which can be used to draw the displacement, velocity and acceleration curves.

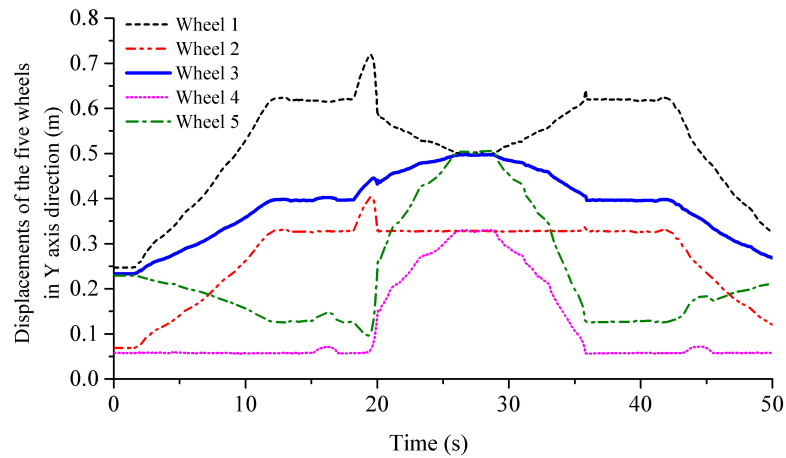


Fig. (11). Curves of displacements of the five wheels in Y axis direction during step-climbing process.

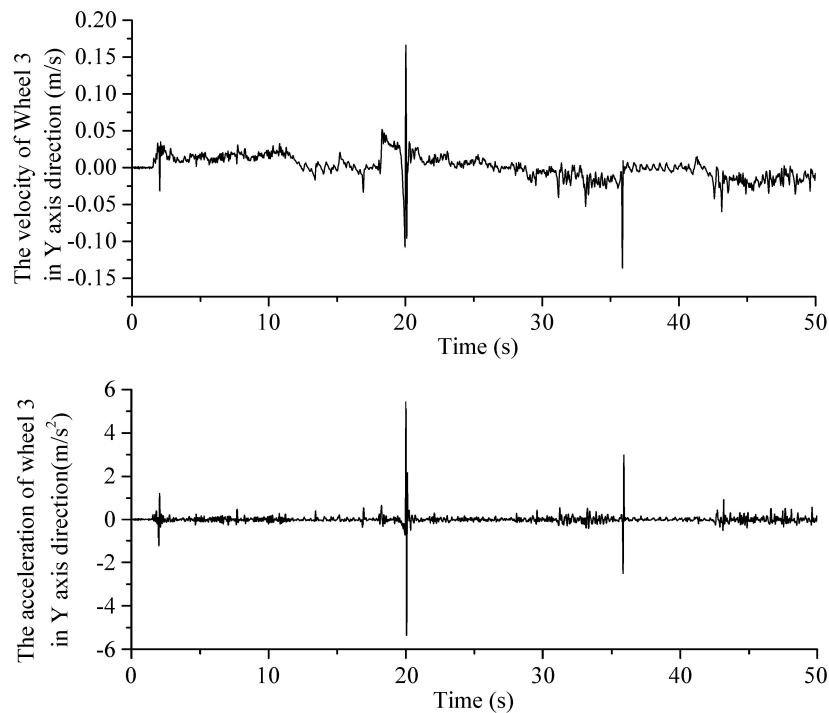


Fig. (12). Curves of the velocity and acceleration of wheel 3 in Y axis direction during step-climbing process.

A three-dimensional coordinate system is established, the coordinate origin is arranged on the ground, and the vertical direction is taken as y axis direction. The curves of displacements of wheel 1, 3, 4 and 5 in Y axis direction on the left track suspension of the robot in step-climbing process is shown in Fig. (11), and the curves in Fig. (11) are very similar to the curves in Fig. (9). Fig. (12) shows curves of the velocity and acceleration of the wheel 3 in Y axis direction. From Fig. (11), Y axis displacement of the wheels increase and decrease suddenly between 18s to 20s, which reflects the process of the center of gravity crossing over the nosing of the step. In this process, the wheel 2 divorces from and touches down on the step's platform again. There is a small mutation on the displacement time curve of wheel 3 during

the period of 18s to 20s. From Fig. (12), the velocity and acceleration of the wheel 3 in Y axis direction appears to change suddenly. Analyzing the wheel 2's axis Y coordinate value curve, the wheel 2 leaves the upper plane in the climbing process, according to the result, we can speculate that the gravity center coordinates of the robot are substantially at point (460, 55), as compared with the theoretical value in Table 2. If the robot's center of mass is moved forward and downward by adjusting the position of the load, the height of the step which the robot can climb up will increase. The maximum tested height of the step which the robot could climb up is 320mm, with the center of gravity coordinates of the robot at point (480, 24.8).

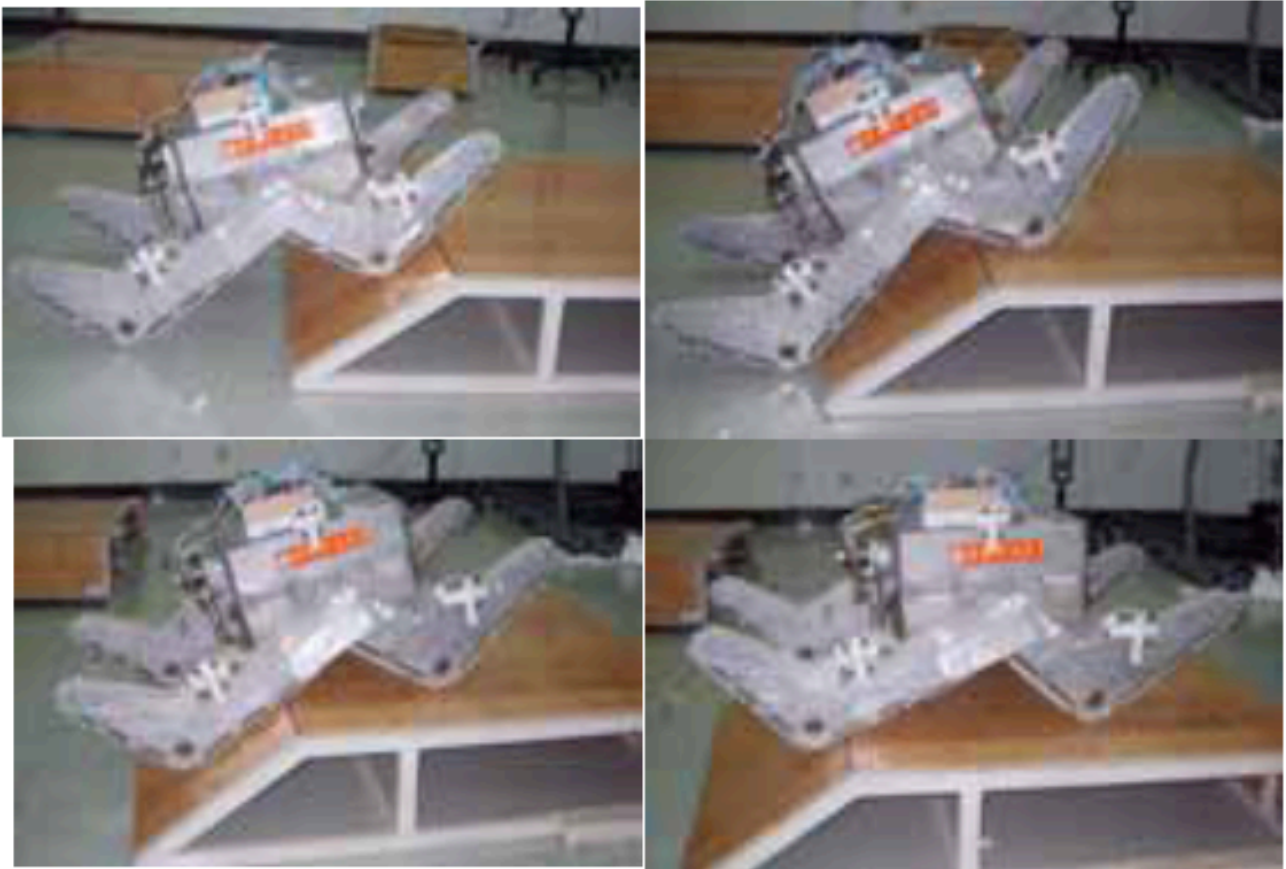


Fig. (13). Slope step-climbing test.

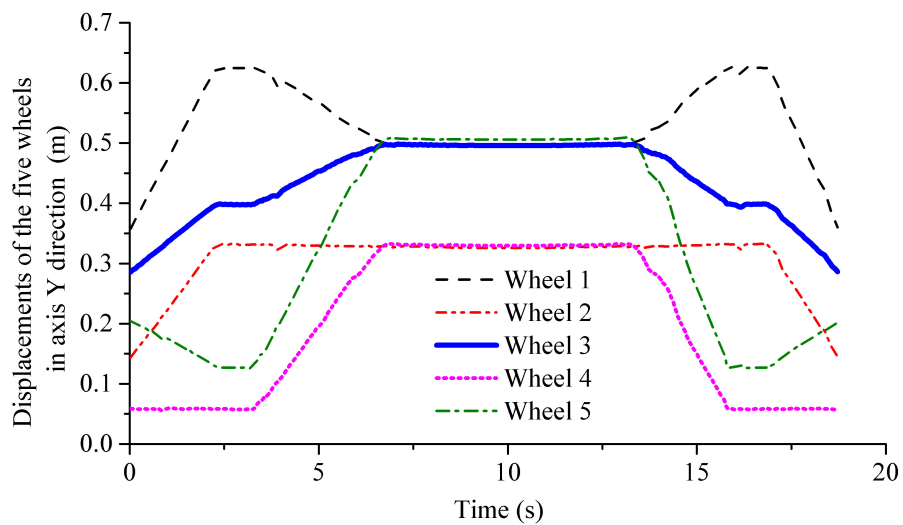


Fig. (14). Curves of displacements of the five wheels in Y axis direction during slope step-climbing process.

4.2.3. Test of Slope Step Climbing

It is very easy for the robot to climb the slope step with a slope between the upper plane and the lower plane. Fig. (13) shows the slope step-climbing process. The robot's front tracks climb the slope and reach on the upper plane, the robot continues to move and the rear tracks climb up the slope.

Fig. (14) shows the curves of displacements of the five wheels in Y axis direction during the slope step-climbing process. Fig. (15) shows curves of velocity and acceleration of the wheel 3 in Y axis direction. The curves indicate that the motion is smoother and the vibration in the process of movement is very small, though the height of the step is the same.

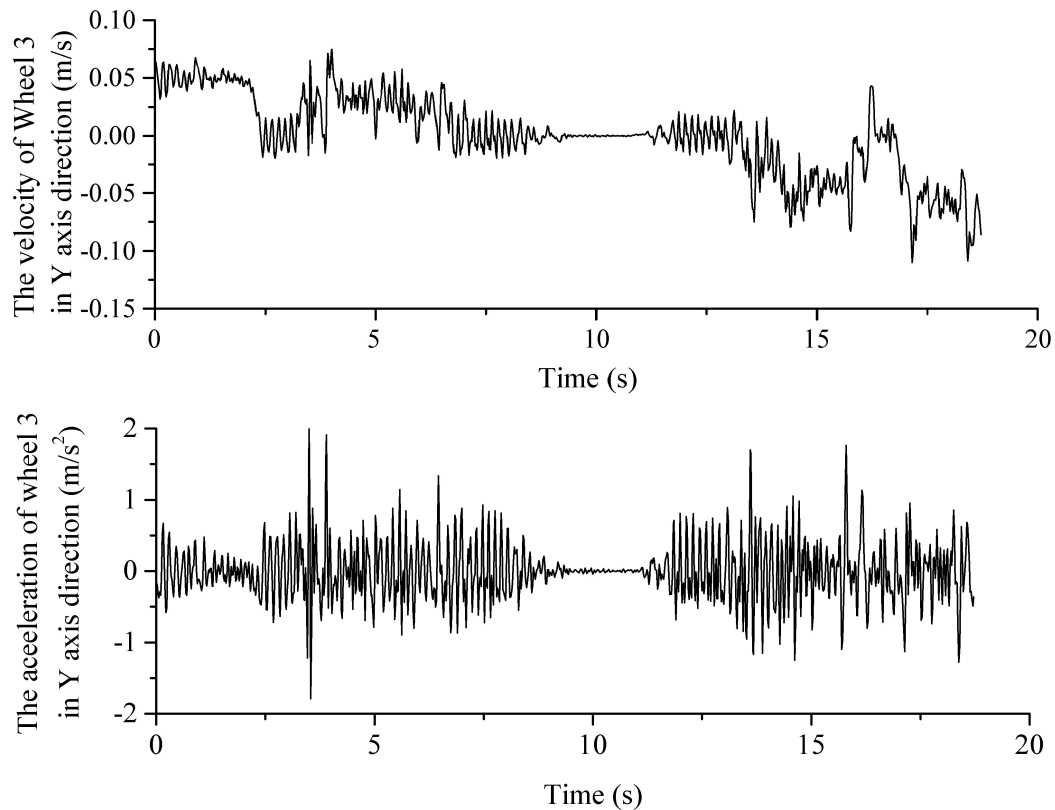


Fig. (15). Curves of the velocity and acceleration of wheel 3 in Y axis direction during slope step-climbing process.

CONCLUSION

In this paper a rocker type asymmetrical W-shaped track robot has been presented, rough terrain adaptation performance of which has been studied in previous researches. In this paper, and the performance of overcoming structured terrain, especially performance of step climbing is analyzed and tested. According to the structure and physical dimensions of the robot and the dimension characteristics of the steps, steps climbing process is analyzed, and the influence of robot's position of center of gravity on the step-overcoming performance is studied.

The 3D models of the robot are imported into the Re-curDyn software, the process of the robot's step climbing is simulated. The curves of the five wheels are obtained during the climbing process. Through the simulation we can understand the change of the robot's attitude to different heights during the step climbing.

A test system for tracking the important positions and motions of the robot has been built in the laboratory using NDI, DMM and a terrain simulation platform. The fixed trapezoidal platform of the terrain simulation platform is used to test the step-climbing, which can provide two kinds of simulated topographies, including a 270 mm high step and a step with a slope. During the test, the important positions and motions of the robot have to be tracked and recorded by the dynamic measurement system. The comparative analysis of the displacement, velocity and acceleration of the five

wheels in independent step and slope step climbing process are carried on.

This work has indicated that W-shaped track mobile robot has a good performance of structured terrain overcoming, and the gravity center position of the robot exercises a great influence on the step-overcoming performance. The step-overcoming performance will improve, if the position of center of gravity is just forward and downward, making it is very easy for the robot to climb the Slope Step because of the guiding role of the slope. In the independent step climbing process, the robot's front track sections of W-shaped track climbs up the nosing of the step firstly, then the rear ones climb. Once robot's position of center of gravity climbs over the nosing, the robot will climb on easily. According to different riser heights and position of center of gravity, there are two situations in the second stage: (1) if the gravity center has been over the nosing when the rear tracks touches the nosing, then the robot rear tracks will climb the steps softly without any impact; (2) if not, then the robot's front tracks will rise from the upper platform, and will fall, causing an impact on the robot.

The robot can easily climb up the steps which are less than 240mm high, and the maximum tested step height is 320mm, but there should be a lower step in front of the step, and the robot's position of center of gravity should be adjusted to a very low and forward position. In short, the W-shaped track mobile robot has a good performance in the structured terrain overcoming.

CONFLICT OF INTEREST

The author confirms that this article content has no conflict of interest.

ACKNOWLEDGEMENTS

This work was financially supported by the Fundamental Research Funds for the Central Universities of China (No.2010QNB18), the China Postdoctoral Science Foundation (No.20110491479), National Natural Science Foundation of China (No. 51205391).

REFERENCES

- [1] Y. W. Li, S. R. Ge and H. Zhu, "Mobile platform of rocker-type coal mine rescue robot", *Mining Sci. Technol. (China)*, vol. 20, no. 3, pp. 466-471, 2010.
- [2] G. Q. Fu, P. Corradi, A. Menciassi and P. Dario, "An integrated triangulation laser scanner for obstacle detection of miniature mobile robots in indoor environment", *IEEE/ASME Transact. Mechatron.*, vol. 16, pp. 778-783, 2011.
- [3] J. Y. Gao, X. S. Gao, J. G. Zhu, W. Zhu, B.Y. Wei, and S. L.Wang, "Coal Mine Detect and Rescue Robot Technique Research", In: *Proc. IEEE Int. Conf. Inform. Automat.*, pp. 1068-1073, 2009.
- [4] R. R. Murphy and J. Kravitz, "Stover Samuel L, Shoureshi Rahmat, Mobile robots in mine rescue and recovery", *IEEE Robot. Autom. Mag.*, vol. 16, pp. 91-103, 2009.
- [5] K. Z. Kenzo, Q. J. Huang, D. S. Komizo and Y. C. Fukao, "Development and control of mine detection robot COMET-II and COMET-III", *JSME Int. J. Series C*, vol. 46, pp. 881-890, 2003
- [6] Y. W. Li, S. R. Ge and H. Zhu, "Deduction of the rocker-type track suspension configurations and their applications to coal mine rescue robots", *Robot(China)*, vol. 32, no. 1, pp. 25-33, 2010.
- [7] Y. W. Li, S. R. Ge and H. Zhu, "Mobile Platform of a Rocker-type W-shaped Track Robot", *Key Eng. Mat.*, vol. 419-420, pp. 609-612, 2010.
- [8] Y. W. Li, S. R. Ge, W. L. Liu and F. Tian, "Analysis and Test on Rough Terrain Adaptation Performance of the Rocker-type W-shaped Track Coal Mine Exploring Robo". *Inform. Technol. J.*, vol. 12, no.14, pp. 2921-2928, 2013.
- [9] Information on <http://industrial.ndigital.com/products/optotrak/optotrak-overview/>
- [10] Y. W. Li, S. R. Ge, X. Wang, and H. B. Wang. "Steps and Stairs-climbing Capability Analysis of Six-tracks Robot with Four Swing Arms", *Appl. Mech. Mat.*, vol. 397-400, pp. 1459-1468, 2013.
- [11] M. L. Liu, J. Zhang and K. Li, "Obstacle performance of track robot with passive rocker based on RecurDyn", *Appl. Mech. Mat.*, Vol. 397-400, pp.1580-1588, 2013.

Received: September 16, 2014

Revised: December 23, 2014

Accepted: December 31, 2014

© Li *et al.*; Licensee Bentham Open.

This is an open access article licensed under the terms of the Creative Commons Attribution Non-Commercial License (<http://creativecommons.org/licenses/by-nc/4.0/>) which permits unrestricted, non-commercial use, distribution and reproduction in any medium, provided the work is properly cited.